Surface Science 602 (2008) 2300–2304

Contents lists available at ScienceDirect

Surface Science

journal homepage: www.elsevier.com/locate/susc

# Vibrational properties of Na nanoclusters self-assembled on Si(1 1 1) surface

C.G. Hwang [a], N.D. Kim [a], S.Y. Shin [a], J.W. Chung [a,*], J.H. Nam [b], M.K. Kim [b], C.-Y. Park [b], J.R. Ahn [b]

[a] Physics Department and Basic Science Research Institute, Pohang University of Science and Technology, San 31 Hyoja Dong, Pohang 790-784, Republic of Korea
[b] Department of Physics and Institute of Basic Science, Sungkyunkwan University, Suwon 440-746, Republic of Korea

ARTICLE INFO

*Article history:*
Received 7 April 2008
Accepted for publication 12 May 2008
Available online 17 May 2008

*Keywords:*
Surface electronic phenomena
Vibrational property
Electron energy loss spectroscopy
Nanocluster
Surface structure

ABSTRACT

We have investigated structural and vibrational properties of Na nanoclusters self-assembled on the Si(1 1 1)-7 × 7 surface at room temperature mainly using high-resolution electron-energy-loss spectroscopy. We observe three characteristic loss peaks $L_1$, $L_2$, and $L_3$ ascribed to an interband transition, a local atomic vibration, and another interband transition from an Na nanocluster-induced state, respectively. The spectral change of $L_1$ with Na coverage $\theta$ suggests that the $S_1$ dangling bond band is gradually filled up to open a band gap with increasing $\theta$ up to 1.1 eV when all three loss peaks completely disappeared. The relatively high loss energy $E_l = 243$ meV of $L_2$ with a narrow linewidth of 32 meV indicates the only Na–Si atomic vibrational mode with Na atoms occupying the tilted on-top sites above Si rest atoms. Furthermore the extremely weak loss peak $L_3$ visible at a coverage range unique only to the Na nanoclusters proves the presence of a Na nanoclusters-induced electronic state $N_2$. These observations provide explanation to most unresolved spectral behavior of earlier photoemission study and evidence for the atomic structure of the Na nanocluster.



Nanoclusters are attractive host for the diverse industrial applications including quantum information processing, optical devices, and biology due to their atomic like electronic properties [1–3]. Various experimental approaches such as lithography, etching, and a method using the periodicity of solid surfaces have been adopted to grow such nanoclusters [4–6]. Recently, several atomic species have been reported to form lattice-like arrays of nanoclusters self-assembled on the Si(1 1 1)-7 × 7 surface at room temperature [7,8,10,11,9].

As reported by Cho and Kaxiras, metal adsorbates occupy high symmetry sites around Si restatoms within the so-called attractive basins to form nanoclusters [12]. Since there are three attractive basins in each faulted half unit cell (FHUC) and unfaulted half unit cell (UHUC), nanoclusters in their stable configurations tend to make a lattice-like array as observed in scanning tunneling microscope (STM) images. Most nanoclusters formed on the Si(1 1 1)-7 × 7 surface are found to be semiconducting and contain six adsorbate atoms in each nanocluster [7,8,10,11,9]. One of the interesting features of such nanoclusters exhibiting atomically well resolved STM images is that most metal adsorbates cause significant rearrangement of the substrate Si atoms upon forming nanoclusters at room temperature (RT) [7,8] although some exceptions have also been reported [10,11,9].

Sodium (Na) nanoclusters, in particular, show some distinct features compared with other nanoclusters [7,13]. Wu et al. reported that there are three regions in the curve of work function change with increasing Na coverage $\theta$ revealing two inflection points at $\theta_1 = 0.08$ monolayers (MLs) and $\theta_2 = 0.22$ ML. For $\theta \leqslant 0.08$ ML, the surface shows a gas-like phase with atomically unresolved STM imgages where Na atoms appear to be quite mobile on the surface. For 0.08 ML $\leqslant \theta \leqslant$ 0.22 ML, Na atoms form nanoclusters with a maximum density at 0.22 ML. Based on their STM observation and theoretical calculations, they proposed an atomic model where each Na nanocluster contains six Na atoms in the form of a triangle surrounding a Si trimer in the middle formed by Si adatoms moved inward (see Fig. 3 in Ref. [7]). Meanwhile Ahn et al. reported angle-resolved photoemission (ARP) study that new surface states associated with Na adsorption appear for each stage of adsorption, and demanded a theoretical calculation of band structure to explain spectral behaviors of these states [13].

With this background, we have investigated properties of electronic excitations associated with the formation of Na nanoclusters on the Si(1 1 1)-7 × 7 surface. We find three characteristic loss peaks in our high-resolution electron energy loss spectroscopy (HREELS) that behave quite differently with $\theta$. The behavior of a peak $L_1$ of loss energy $E_l = 300$ meV apparently stemming from an interband transtion from $S_1$ state near Fermi level persists until the completion of the array of Na nanoclusters at $\theta_2$. Meanwhile another loss peak $L_2$ of $E_l = 243$ meV changes sensitively with $\theta$ showing a quite narrow linewidth of 32 meV. We ascribe $L_2$ to the atomic vibration of Na atoms occupying the on-top sites above

* Corresponding author. Tel.: +82 54 2792071; fax: +82 54 2793099.
*E-mail address:* jwc@postech.ac.kr (J.W. Chung).
URL: http://www.postech.ac.kr/phys/snpl/ (J.W. Chung).

0039-6028/$ - see front matter © 2008 Elsevier B.V. All rights reserved.
doi:10.1016/j.susc.2008.05.011

Si restatoms. Another loss peak $L_3$ appears to be quite weak and is ascribed to an interband transition from the Na nanoclusters-induced state $N_2$. The presence of these loss peaks and their spectral behaviors with $\theta$ explain qualitatively most of the unresolved spectral features in previous ARP study [13]. In addition, the only atomic vibrational mode $L_2$ observed in our EELS spectra confirms the atomic model proposed by Wu et al., and explains the rather quick disappearance of $S_2$ state in earlier ARP study.

Experiments have been performed in two separated ultra-high vacuum chambers of STM and HREELS equipped with typical surface diagnostic probes such as low energy electron diffraction (LEED) and X-ray photoemission spectroscopy (XPS). The base pressure of the chambers has been maintained below $1 \times 10^{-10}$ mbar during the whole experimental process. The EELS has a Leybold-Heraeus ELS-22 spectrometer constituted with two 127° cylindrical deflectors for both monochromator and analyzer, which yields an optimum resolution of 7 meV and a half-acceptance angle of 2°. The XPS primarily used to measure work function change induced by Na adsorption utilizes a concentric hemisphere analyzer and an X-ray source of Mg Kα radiation. A Si(1 1 1) sample was prepared by cutting a n-doped Si wafer of a resistivity $\sim 2\Omega$ cm into a ribbon shape of dimensions $5 \times 30 \times 0.5$ mm$^3$. We have followed a well-known cleaning recipe of the sample until we observe a well-defined $7 \times 7$ LEED pattern with a dark background showing no detectable impurity peaks (O 1s, C 1s) in XPS scan [14]. We have used a commercial Na SAES getter source to deposit Na atoms onto the clean Si(1 1 1)-$7 \times 7$ surface. The Na deposition has been made at a deposition rate of 0.018 ML/min after 5 min cooling from annealing at 800 °C to ensure the adsorption of Na atoms at RT. The Na coverage has been calibrated by measuring work function change. All EELS measurements have been performed within one hour after cleaning the sample to avoid any contamination effect.

As shown in Fig. 1, we have also observed three different phases of Na nanoclusters upon forming on the Si(1 1 1)-$7 \times 7$ surface at RT as reported by Wu et al. [7]. The sparse distribution of Na nanoclusters at $\theta \leqslant \theta_1$ is seen in Fig. 1a with most Na nanoclusters occupying FHUCs. With increasing $\theta$, we find a lattice-like array of nanoclusters at $\theta_2$ (Fig. 1c). With further deposition of Na, the nanoclusters appear to decay into a nonuniform distribution of clusters with deformed shapes (Fig. 1d). Our work function change versus $\theta$ curve ($\Delta\phi$) shown in Fig. 2 also exhibits two infection points at $\theta_1$ and $\theta_2$ as observed by Wu et al. [7]. The three different stages I, II, and III as distinguished by different slopes and also different STM images in Fig. 1 illustrate the different phases of forming nanoclusters. The stage I identified as a gas-like phase reveals a rapid linear drop of work function as mostly seen from atomic adsorption on metal surfaces due to the formation of electric dipole moments on the surface. Ahn et al. observed that a new state $N_1$ of binding energy $E_b = 0.36$ eV develops in the stage I and its binding energy continues to shift to higher energy side up to $E_b = 0.56$ eV with increasing $\theta$. They also observed that the surface state $S_2$ stemming from Si restatoms weakens quickly with $\theta$ while $S_1$ from Si adatoms and $S_3$ from adatom backbonds slowly weaken. With the formation of Na nanoclusters in the stage II, $\Delta\phi$ shows a much slower decrease with $\theta$ where new surface states $N_2$ of $E_b = 0.50$ eV and $N_3$ of $E_b = 1.10$ eV appear in photoemission spectra [13].

We present a series of HREELS spectra obtained from the Na adsorbed surface at various values of $\theta$ in Fig. 3. The spectra have been measured with a primary electron energy of 5.0 eV in a specular scattering geometry with incidence angle $\theta_i = 60°$. The bottom spectrum shows a Drude tail of metallic continuum due to the continuous electron-hole pair excitations from the $S_1$ state near Fermi level [15]. As soon as Na is adsorbed, the surface, however, becomes semiconducting as seen by the significantly reduced linewidth of the elastic peak at low $\theta$ (not shown). The surface eventually shows a band gap of 1.1 eV near 0.5 ML as reported earlier [14]. Interestingly we notice a quite broad bump centered around a loss energy $E_l = 300$ meV from the clean Si(1 1 1)-$7 \times 7$ surface at 2° off from the specular angle (the second spectrum from the bottom in Fig. 3). This broad feature may be a loss peak produced by different scattering mechanism such as impact scattering [16]. As discussed later it, however, appears to survive with Na adsorption almost up to $\theta_2$ where Na nanoclusters completely cover the whole surface. The most prominent loss peak associated with Na in Fig. 3 is the sharp loss peak with loss energy of 243 meV, which sensitively changes with $\theta$. The spectrum shown in inset also show a new loss peak centered at 622 meV at $\theta = 0.282$ ML, unique only to the Na nanoclusters.

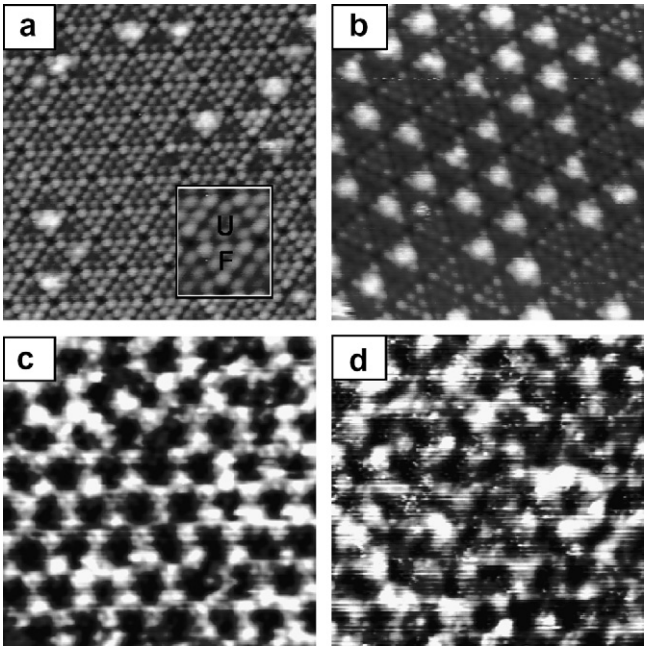


**Fig. 1.** STM images of the Na adsorbed Si(1 1 1)-$7 \times 7$ surface at RT with coverage (a) 0.04 ML, (b) 0.12 ML, (c) 0.22 ML, and (d) 0.33 ML. Faulted and unfaulted halves of a Si(1 1 1)-$7 \times 7$ unit cell are denoted by "F" and "U", respectively, in inset of (a). One finds that the sparse distribution of Na nanoclusters in (a) and (b) becomes a lattice-like array in (c).

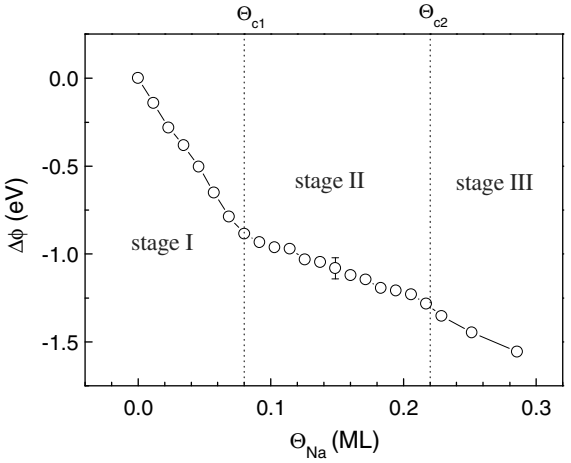


**Fig. 2.** Work function change ($\Delta\phi$) versus Na coverage ($\theta$). There are three distinct stages I, II, and III corresponding to gas-like phase, lattice-like phase, and decayed phase of nanoclusters, respectively, as suggested by a previous STM study (Ref. [7]).

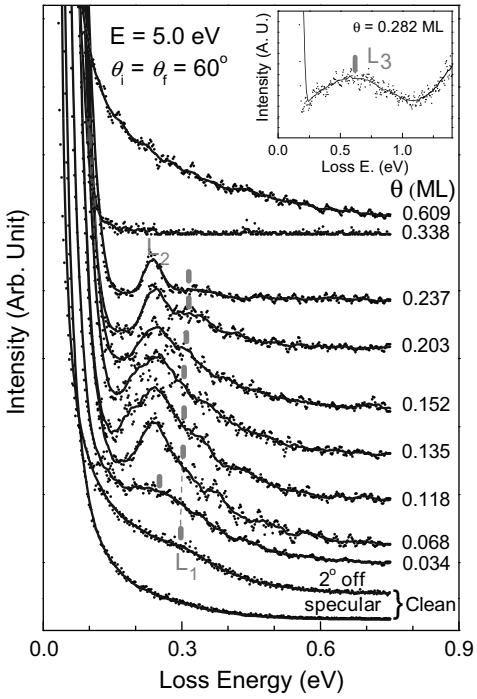


**Fig. 3.** Spectral change of HREELS spectra with increasing Na coverage $\theta$. The spectra have been measured with a primary electron energy of 5.0 eV at a specular geometry with incidence angle $\theta_i = 60°$. The loss peak $L_1$ and $L_2$ attributed to an interband transition (marked by vertical bars) and a local atomic vibration, respectively (see text). Inset shows the spectrum at $\theta = 0.282$ ML where a new loss peak $L_3$ at 0.622 eV is apparent.

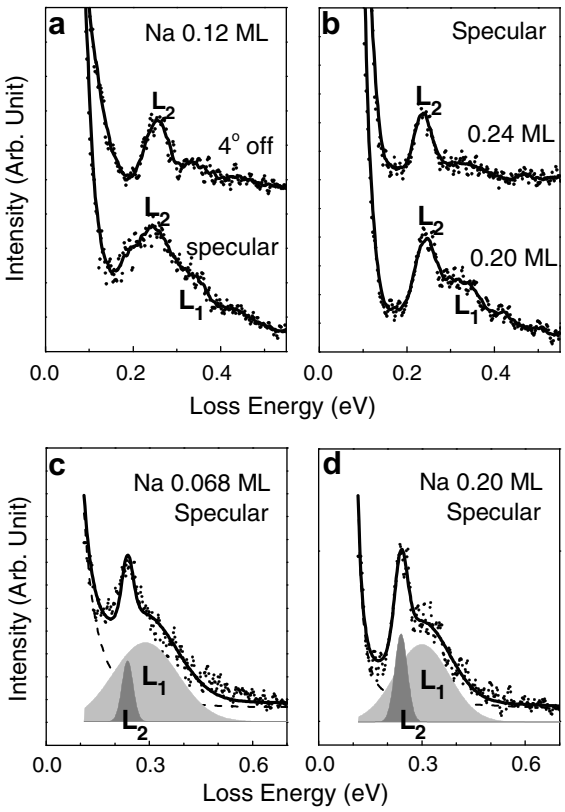


**Fig. 4.** Spectral changes measured at different scattering angles (a) and different coverages (b). The spectra at two different coverages have been fitted with two Gaussian peaks to find a broad ($L_1$) and a narrow ($L_2$) loss peaks in (c) and (d).

In order to identify the origin of the loss features in Fig. 3, we have examined the spectral changes as a function of scattering angle and $\theta$ as shown in Fig. 4. In Fig. 4a, the broad loss feature associated with Na adsorption is found to consist of two loss peaks $L_1$ and $L_2$ as apparently seen by the much reduced $L_1$ peak at 4° off specular scattering geometry at $\theta = 0.12$ ML. Even at specular geometry, the $L_1$ peak weakens its intensity with increasing $\theta$ and becomes almost disappeared at $\theta = 0.24$ ML leaving only the sharp loss peak $L_2$ of $E_l = 243$ meV (Fig. 4b). In order to quantify our HREELS spectra, we have fitted a loss spectrum with two loss peaks of Gaussian shapes after subtracting the inverse polynomial background as done earlier [17]. We have shown the fitted spectra at $\theta = 0.068$ ML for the stage I in Fig. 4c and $\theta = 0.20$ ML for the stage II in Fig. 4d.

Our fit results show that while $L_1$ changes sensitively with $\theta$ as seen in Fig. 5, $L_2$ remains almost unchanged at $E_l = 243$ meV within the experimental error range. We now discuss where these loss peaks come from. Since $L_1$ has a linewidth greater than 160 meV, much wider than the typical width of local atomic vibrations ($\leqslant$25 meV) and its loss energy much higher than the upper limit of optical phonons of Si crystal ($\sim$57 meV), we safely exclude the possibilities of atomic vibrational origin as well as of phonon [18]. We also rule out a plasmon excitation due to the small electron concentration in Na nanoclusters. Since $L_1$ remains with Na adsorption up to $\theta_2$ before disappearing completely above $\theta_2$, we attribute $L_1$ to an interband transition closely related with Na nanoclusters.

The fact that $L_1$ is observed even from the clean surface suggests that it is an interband transition from the surface state $S_1$ just below Fermi level to an empty state in the conduction band of the clean surface. Although this transition is hidden in the Drude tail for the clean surface, it begins to show up as the Drude tail becomes significantly suppressed by Na adsorption (see inset

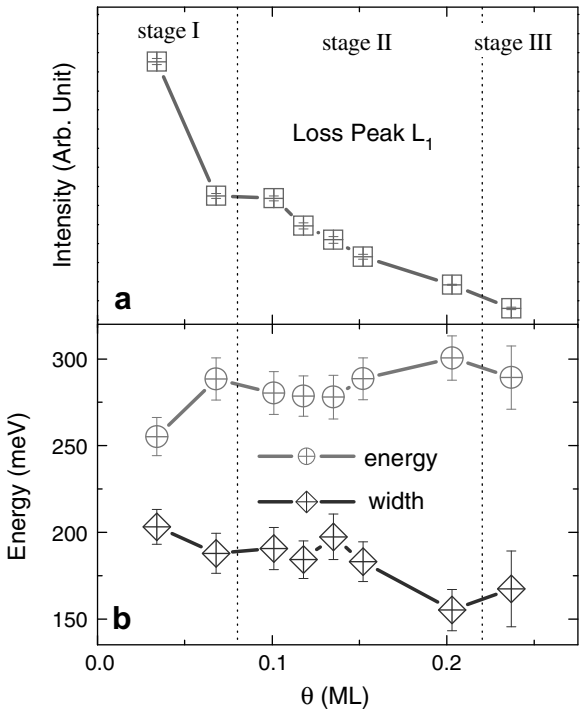


**Fig. 5.** Na coverage dependence of (a) intensity and (b) loss energy as well as the linewidth of $L_1$. One notices distinct behaviors for the two stages I and II of Na adsorption.

of Fig. 3). The change of loss energy of $L_1$ in Fig. 5 thus reflects the change of band gap illustrated by the change of linewidth of elastic peak in Fig. 3. Such a change of band gap with $\theta$ may be

understood by the reduced density of states near Fermi level as the dangling bonds of Si adatoms are occupied by the charges from Na adatoms. Since $L_1$ decreases but remains finite throughout the formation of Na nanoclusters, there must be Si dangling bonds intact from Na adsorption. This is consistent with the decreasing but finite intensity of $L_1$ in Fig. 5a although it becomes very weak at high coverage near $\theta_2$. This feature of $L_1$, however, is inconsistent with the nearly vanishing $S_1$ state at early stage of adsorption in photoemission data probably due to matrix element effects causing the photon energy dependence of the signal [13]. Although the opening of band gap with the formation of nanoclusters have been also reported for aluminum, indium and Na nanoclusters, such a sensitive change of $S_1$ state has not been quantitatively measured in previous studies [19,13].

Another broad loss feature $L_3$ shown in inset of Fig. 3 can only be ascribed to an interband transition from the $N_2$ band observed at energy 0.5 eV below Fermi energy in earlier photoemission data [13]. It is noteworthy, however, that no other loss peaks associated with new surface states $N_1$, $N_3$, and $N_4$ induced by Na up to stage II in photoemission study [13] appears in our HREELS spectra in Fig. 3. This might reflect the matrix element effect or non-dipolar electrons scattering for the interband transitions involving the new states. As $\theta$ exceeds $\theta_2$, the Na nanoclusters begin to decay as seen in STM image of Fig. 1d for $\theta = 0.33$ ML. The surface becomes more semiconducting with increasing $\theta$ until it shows a band gap of 1.10 eV with loss peaks $L_1$, $L_2$, and $L_3$ completely quenched as reported earlier [14]. Further dose of Na makes the surface metallic again by the Na overlayer as seen by the reappearance of a Drude tail.

As discussed below, the presence of $L_2$ in Fig. 3 provides an important clue that the Na nanoclusters has an atomic structure suggested earlier by Wu et al. sketched in Fig. 6. Since $L_2$ has a loss energy $E_l = 243$ meV much higher than the maximum phonon energy of the surface together with a narrow linewidth of 32 meV, it should represent one of dipole-active atomic vibrational modes rather than an interband transition. Apparently the same peak P1 has mistakenly identified as an interband transition probably due to the relatively poor resolution obtained at specular direction in previous work [14]. Furthermore since $L_2$ rapidly disappears with the decay of Na nanoclusters above $\theta_2$, $L_2$ must be associated closely with a local atomic vibration of Na nanoclusters.

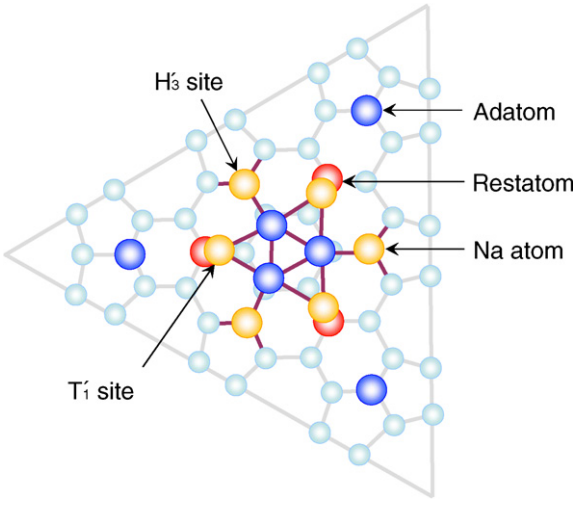


**Fig. 6.** Atomic arrangement of a Na nanocluster proposed by Wu et al. (Ref. [7]). The Na nanocluster consists of six Na adatoms (orange spheres) surrounding the central Si trimer (blue spheres) shifted inward by Na adsorption. Note that three Na adatom occupy the tilted on-top sites ($T_1'$) above Si rest atoms (red spheres) while another three the slightly shifted hollow sites ($H_3'$). Na–Si bondings are drawn by purple bars. (For interpretation of the references in color in this figure legend, the reader is referred to the web version of this article).

The proposed atomic model by Wu et al. in Fig. 6 shows that a Na nanocluster consist of six Na atoms surrounding the central Si trimer. One may think of several atomic vibrations from this structural model including the Si–Si vibrations of the trimer and Na–Si vibrations. $L_2$ is not likely to come from the Si trimer since there are three normal modes of vibration for a equilateral triangular structure with lowest energy of about 22 meV for a Si trimer [16]. One then notices that there are two different Na–Si bondings with Na occupying the $H_3'$ sites slightly off from the three-fold hollow sites $H_3$ and the slightly tilted on-top sites $T_1'$ above Si rest atoms. We also remind that local vibrational frequency tends to decrease with increasing coordination number as seen from the vibrational energies of 217, 165, and 77 meV for hydrogen atom occupying the on-top, bridge, and hollow sites, respectively [20]. Since the stretching mode of H–Si vibration adsorbed at on-top site has a vibrational energy of 250 meV [21], it becomes reasonable to assign $L_2$ as a stretching mode of Na–Si vibration with Na sitting at the tilted on-top sites ($T_1'$) in Fig. 6. We also rule out the possible Si–O vibration of energy 140 meV for $L_2$ due to the oxygen contamination of the surface [22] although alkali metals are known to promote oxidation of Si surface [23].

It might be instructive to think why more massive Na–Si stretching mode has about the same vibrational energy (240 meV) with that of H–Si stretching mode. Considering the different reduced masses of the two bondings it may simply implicate that the Na–Si bonding of a Na nanocluster is twelve times stronger than the H–Si bonding, which is the ratio of reduced masses of the two bondings. Such a strong Na–Si bonding may the reason why we find dents at the places where Na atoms were removed by STM tip [24]. The somewhat high vibrational energy of $L_2$ may also reflect the meta-stable nature of a Na nanocluster at RT since the ground state of the Na adsorbed Si(1 1 1) surface with similar Na coverage exhibits a unique $3 \times 1$ structure typical of group I elements [25].

In summary, three characteristic loss peaks $L_1$, $L_2$, and $L_3$ observed in our HREELS spectra obtained from the Na adsorbed Si(1 1 1) surface at RT are ascribed to an interband transition, a local Na–Si atomic vibrational mode, and another interband transition from $N_2$ state unique only to the Na clusters. The spectral behavior of $L_1$ associated with interband transition reveals the gradual opening of band gap with Na adsorption by filling the dangling bonds of $S_1$ surface state near Fermi level. Such interpretation is qualitatively consistent with the spectral changes of surface states ($S_1$ and $S_3$) observed in photoemission study considering the much sensitive probing ability of HREELS. The loss peak representing the Na–Si stretching mode suggests that Na atoms occupy slightly tilted on-top sites above Si rest atoms, which is the only sites that produces a single atomic vibrational mode as observed. This explains why $S_2$ state stemming from Si rest atoms quickly vanishes with Na adsorption in previous photoemission study. We further show that an interband transition from the Na cluster-induced electronic state $N_2$ is, although very weak, observed in this study. Our HREELS observations appear to be consistent with spectral behaviors of surface states in photoemission upon adsorption of Na and also confirm the structural model proposed earlier.

## Acknowledgements

This work was supported by the Korea Research Foundation, Grant funded by the Korean Government (MOEHRD, Basic Research Promotion Fund) (KRF-2006-312-C00513).

## References

[1] X. Li, Y. Wu, D. Steel, D. Gammon, T.H. Stievater, D.S. Katzer, D. Park, C. Piermarocchi, L.J. Sham, Science 301 (2003) 809.

[2] R.E. Bailey, A.M. Smith, S. Nie, Physica E 25 (2004) 1.
[3] B. Dubertret, P. Skourides, D.J. Norris, V. Noireaux, A.H. Brivanlou, A. Libchaber, Science 298 (2002) 1759.
[4] J. Sone et al., Nanotechnology 10 (1999) 135.
[5] S. Facsko, T. Dekorsy, C. Koerdt, C. Trappe, H. Kurz, A. Vogt, H.L. Hartnagel, Science 285 (1999) 1551.
[6] H. Brune, M. Giovannini, K. Bromann, K. Kern, Nature 394 (1998) 451.
[7] K. Wu et al., Phys. Rev. Lett. 91 (2003) 126101.
[8] Y.P. Zhang, L. Yang, Y.H. Lai, G.Q. Xu, X.S. Wang, Surf. Sci. 531 (2003) L378.
[9] J.-L. Li et al., Phys. Rev. Lett. 88 (2002) 066101.
[10] J. Jia, J.-Z. Wang, X. Liu, Q.-K. Xue, Z.-Q. Li, Y. Kawazoe, S.B. Zhang, Appl. Phys. Lett. 80 (2002) 3186.
[11] H.H. Chang, M.Y. Lai, J.H. Wei, C.M. Wei, Y.L. Wang, Phys. Rev. Lett. 92 (2004) 066103.
[12] K. Cho, E. Kaxiras, Surf. Sci. 396 (1998) L261.
[13] J.R. Ahn, G.J. Yoo, J.T. Seo, J.H. Byun, H.W. Yeom, Phys. Rev. B 72 (2005) 113309.
[14] K.D. Lee, J.R. Ahn, J.W. Chung, Appl. Phys. A 68 (1999) 115.
[15] R. Losio, K.N. Altmann, F.J. Himpsel, Phys. Rev. B 61 (2000) 10845.
[16] H. Ibach, D.L. Mills, Electron Energy Loss Spectroscopy and Surface Vibrations, Acedemic Press, New York, 1982.
[17] P. Laitenberger, R.E. Palmer, Phys. Rev. Lett. 76 (1996) 1952.
[18] U. Harten, J.P. Toennies, Ch. Wöll, L. Miglio, P. Ruggerone, L. Colombo, G. Benedek, Phys. Rev. B 38 (1988) 3305.
[19] L. Zhang, S. Zhang, Q. Xue, J. Jia, E. Wang, Phys. Rev. B 72 (2005) 033315.
[20] D. Tománek, S.G. Louie, C.-T. Chan, Phys. Rev. Lett. 57 (1986) 2594.
[21] G. Lucovsky, J. Vac. Sci. Technol. 16 (1979) 1225.
[22] S. Fujimura, K. Ishikawa, H. Ogawa, J. Vac. Sci. Technol. A 16 (1998) 375.
[23] G. Lee, E.-J. Cho, Y. Park, S. Cho, H.-G. Lee, Surf. Sci. 501 (2002) L177. and references therein.
[24] Kehui Wu, Y. Fujikawa, T. Briere, V. Kumar, Y. Kawazoe, T. Sakurai, Ultramicroscopy 105 (2005) 32.
[25] J.R. Ahn, N.D. Kim, S.S. Lee, K.D. Lee, B.D. Yu, D. Jeon, K. Kong, J.W. Chung, Europhys. Lett. 57 (2002) 859.